

DYNAMIC ENERGY ABSORPTION MODES OF BRAIDED CARBON/VINYL ESTER COMPOSITE CRUSH TUBES

Thomas J. Brimhall, PhD, PE

Altair Engineering

Abstract

Energy absorption of fiber reinforced composite structures is of interest to the automotive industry as their specific energy absorption, (SEA), i.e. the energy absorption capability per unit mass, is higher than many metallic counterparts. The SEA of composite structures has been observed to decrease under dynamic crush loading when compared with quasi-static compression. The observed energy absorbing modes include tube corner splitting, composite delamination, matrix damage due to bending, and sliding friction of the composite with a plug type crush trigger.

Corner splitting was estimated to absorb less than 1% of the total energy absorbed. Energy absorption attributable to delamination was estimated to be 2.8% of the crush tube SEA. The SEA attributable to matrix damage from bending was 62.2% for quasi-static loading and 78.1% under dynamic loading. The percentage of total SEA attributable to sliding friction between the plug type trigger and composite tube was 34.8% under quasi-static loading and 18.1% under dynamic loading.

The decrease in sliding friction SEA of 6.3 J/gm accounted for nearly all of the decrease in crush tube SEA of 6.6 J/gm between dynamic crush and quasi-static compression. Sliding friction was concluded to be responsible for the decrease in overall tube SEA when compression loaded at a quasi-static rate vs. a dynamic rate.

Introduction

Energy absorption modes observed during axial loading were corner splitting, composite delamination, and matrix damage in the sides of the composite tube [1]. In addition, friction energy absorption was inferred by observing composite sliding over the crush trigger. Several researchers have speculated as to the relative energy absorption attributable to friction to be from of secondary importance [2] to as high as 50% [3,4]. Experimental data measuring sliding friction is needed to more completely characterize the mechanisms of composite energy absorption. In this paper, simple experimental testing was used to isolate and measure energy absorption by individual modes. Energy absorption attributable to corner splitting was estimated based on a standard tensile test. Delamination energy absorption was estimated using end notch flexure test data. Matrix damage due to bending and friction energy absorption was measured using a strip test fixture developed by the author.

Material Testing

Material property tests were conducted on the carbon fiber composite to characterize the selected test material. Plaques were fabricated at the same time as the crush tubes and were used for materials characterization. Plaque characterization testing was performed by Delsen Testing Laboratories in Glendale, California. Fiber and resin weight content for the carbon fiber composites was determined using method ASTM D2584 [5]. The carbon/vinyl ester composite

architecture is presented in Table I.

Table I Composite plaque characteristics.

Reinforcement	Matrix	Architecture	Fiber Content (wt. %)	Fiber Volume (%)	Laminate Density (gm/cm ³)
Carbon Fiber Fortafil 503 80k Axial Grafil 12k Off-Axis	Ashland Hetrion 922 Vinyl Ester	Tri-axial Braid [0/±45] ₄	54.5	43.0	1.419

Carbon fiber composite characterization test results are presented in [Ref. 6] and summarized in Table II. A typical carbon fiber tensile load-displacement plot in the 90° direction is presented in Figure 1. The curve is nearly linear up to material fracture indicating that there is little energy absorption due to plastic deformation.

Table II Carbon fiber plaque composite mechanical properties.

Direction	Stress, Max (MPa)	Modulus (GPa)	Poisson's Ratio	Strain, Max (%)	Fracture Energy (J/cm ³)
Tensile					
0°	654	60.33	0.562	1.08	3.623
90°	65.2	8.756	0.109	1.20	0.475
Compressive					
0°	376	59.71	--	0.66	1.289
90°	91.7	10.06	--	0.89	0.404
ShortBeam Shear					
	43.1				
Strain Energy Release Rate	G_{IIc} (J/cm ²)				
	0.159				
Physical Properties	Density (gm/cm ³)	Fiber Weight Content (%)	Resin Weight Content (%)		
Fiber	1.80				
Resin	1.14				
Composite	1.42	54.74	45.26		

90T11

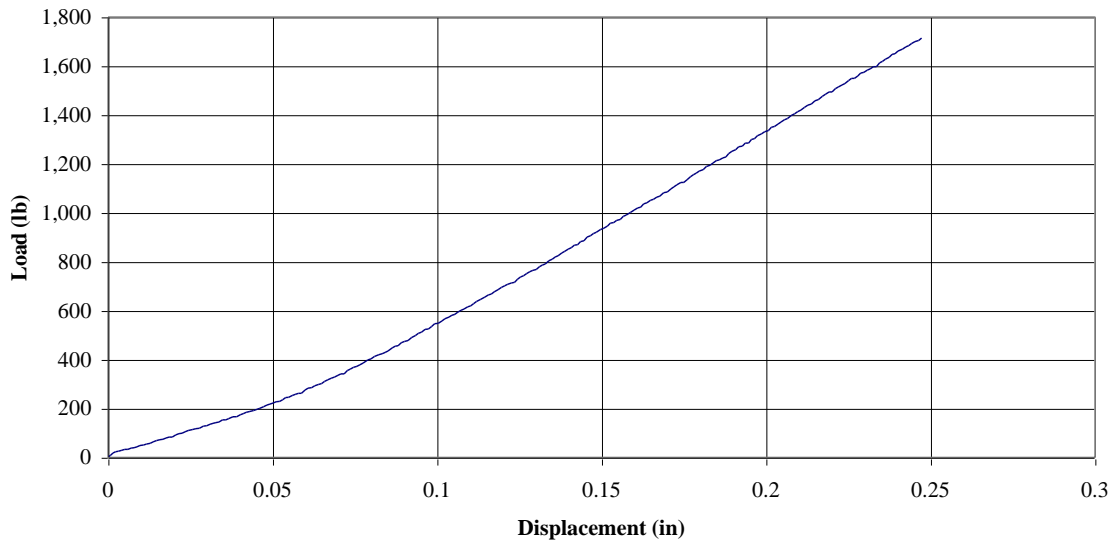


Figure 2 Typical carbon fiber composite 90° tensile load-displacement curve.

Static Crush Tube Tests

All static crush tube testing was performed at the Ford Scientific Research Laboratory using an MTS 810 (servo hydraulic) material test system at ambient room conditions. The MTS load frame has a 222 KN (50,000 lb.) capacity and uses a 22.2 KN (5,000 lb.) load cell. All specimen testing and data was controlled, recorded and analyzed through the use of the SinTech software package, Test Works, on a Dell personal computer. The crosshead speed was 0.0508 m/min.

Five carbon composite tubes were tested with the standard plug type trigger with a fillet radius of 6 mm (Figure 2). The trigger for each composite tube was machined to fit inside the tube with a tolerance of 1 mm or less. The upper end of the tube was contacted directly by the upper platen and was not constrained from movement transverse to the axis of the crush tube. The plug trigger was placed on the lower platen and was also unconstrained from transverse displacement. A schematic of the tube crush testing is presented in Figure 3. In all cases, no transverse displacement of either end of the crush tube was observed. The quasi-static test results are presented in Table III.

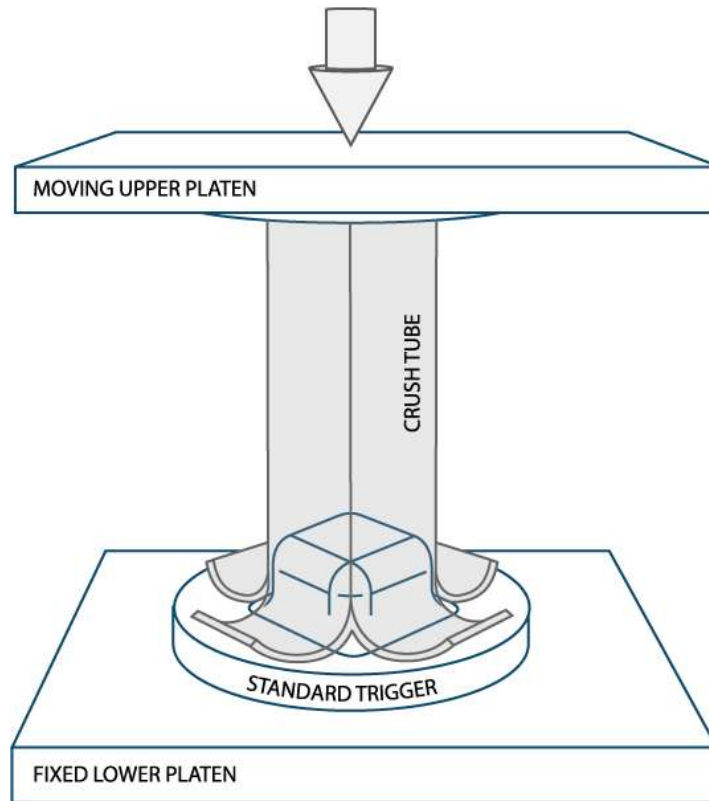


Figure 3 Tube crush test schematic.

Table III Carbon fiber composite crush tube SEA, quasi-static loading rate (0.0508 m/min).

Coupon	Ave. Cross Section Area (cm ²)	Max. Load (N)	Ave. Load (N)	Crush Distance (cm)	Total Energy Absorbed (J)	SEA (J/gm)
4278-2-1	5.26	22,300	18,170	2.4	2,250	24.3
4278-2-4	4.88	28,130	21,450	12.4	2,660	30.9
4278-2-5	4.91	29,390	23,320	12.4	2,890	33.3
4278-2-9	4.93	27,590	22,260	12.4	2,760	31.7
4278-2-17	4.92	29,210	22,330	12.4	2,770	31.9
Ave.	4.98	27,320	21,510	12.4	2,670	30.4

Note: SEA based on material density of 1.42 gm/cm³.

Dynamic Carbon Fiber Composite Crush Tube Tests

Dynamic testing was performed using the Test Machine for Automotive Crashworthiness (TMAC) located at the National Transportation Research Center, Oak Ridge National Laboratory, Tennessee. The Oak Ridge National Laboratory (ORNL) and the Automotive Composites Consortium (ACC) collaborated to define specifications for a unique experimental apparatus that mitigates the shortcomings of existing equipment. MTS Systems Corporation designed and built the servo-hydraulic test machine, referred to as the TMAC. The TMAC, Figure 4, is uniquely capable of conducting controlled progressive crush tests at constant velocity in the intermediate velocity range (i.e., less than 5m/s).

Carbon Fiber Composite Crush Tube Dynamic Test Results

The dynamic test results for the carbon fiber composite are presented in Table IV. A typical dynamic load-displacement plot is presented in Figure 5. Note that the average plateau load is lower for the dynamic loaded carbon fiber composite, 15,650 N, than the same material loaded quasi-statically, 21,510 N. The average SEA for dynamic loading was 23.8 J/gm vs. 30.4 J/gm for quasi-static loading, a decrease of 6.6 J/gm.

Table IV Carbon fiber composite crush tube SEA dynamic loading.

Coupon	Load Rate (m/sec)	Ave. Cross Section Area (cm ²)	Max. Load (N)	Ave. Load (N)	Crush Distance (cm)	Total Energy Absorbed (J)	SEA (J/gm)
4278-2-2	2.0	4.68	20,620	16,110	26.6	4,280	24.2
4278-2-3	2.0	4.84	22,060	16,100	26.8	4,330	23.5
4278-2-11	2.0	4.51	20,040	15,340	26.9	4,130	24.0
4278-2-12	2.0	4.53	20,890	15,030	27.3	4,100	23.4
4278-2-16	2.0	4.65	22,130	15,680	27.1	4,250	23.8
Ave.		4.64	21,150	15,650	26.9	4,220	23.8

Notes: SEA based on material density of 1.42 gm/cm³.



Figure 4 TMAC installation at NTRC.

Table IV Carbon fiber composite crush tube SEA dynamic loading.

Coupon	Load Rate (m/sec)	Ave. Cross Section Area (cm ²)	Max. Load (N)	Ave. Load (N)	Crush Distance (cm)	Total Energy Absorbed (J)	SEA (J/gm)
4278-2-2	2.0	4.68	20,620	16,110	26.6	4,280	24.2
4278-2-3	2.0	4.84	22,060	16,100	26.8	4,330	23.5
4278-2-11	2.0	4.51	20,040	15,340	26.9	4,130	24.0
4278-2-12	2.0	4.53	20,890	15,030	27.3	4,100	23.4
4278-2-16	2.0	4.65	22,130	15,680	27.1	4,250	23.8
Ave.		4.64	21,150	15,650	26.9	4,220	23.8

Notes: SEA based on material density of 1.42 gm/cm³.

Tube 4278-2-12

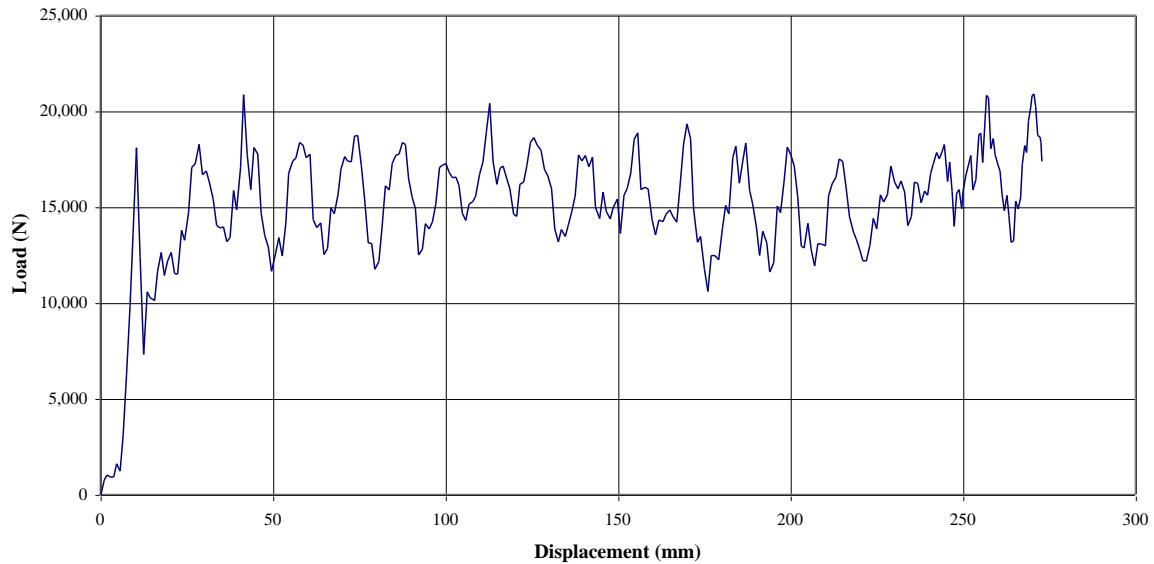


Figure 5 Typical carbon fiber crush tube dynamic load-displacement plot.

Macroscopic Damage Modes

As a tube is crushed, several modes of energy absorption are evident. Delamination, fiber and resin fracture, damage due to bending, and sliding friction of the composite against the plug trigger or platen were observed. Each of these energy absorption modes absorbs varying amounts of energy depending on crush speed, environmental conditions, and composite composition.

During a quasi-static or dynamically loaded tube crush test interlaminar shear loads occur when the composite is forced to bend over the fillet transition between the plug and base plane of the plug trigger that is perpendicular with the crush tube axis and crush direction. Delamination occurs when layers, or plies, of composite separate due to interlaminar shearing forces.

A photo of a quasi-statically compressed carbon fiber composite crush tube is presented in Figure 6. A photo of a dynamically compressed carbon fiber composite crush tube is presented in Figure 7. Careful examination shows two plies present in the damaged carbon fiber composite consistent with the fiber architecture of the carbon fiber composite. The appearance of the quasi-statically compressed and dynamically compressed carbon fiber composite crush tubes are visually similar and suggest similar energy absorption modes. These are: fiber fracture at the tube corners, delamination, and matrix damage.

During crush, the damage process zone advances intermittently as fibers are broken and fiber bundles fracture. Cracks advance to the next fiber or fiber bundle and crack propagation is arrested until the forces due to crush loading become greater than the strength of the fibers. Tensile forces pull the composite material apart at the corners as the tube is forced over the trigger. The increasing perimeter of the trigger that the composite tube is forced over loads the composite in tension similar to the tensile loading imposed during a tensile test of a flat coupon. In the case of the composite tube, this tensile loading is perpendicular, or 90° , to the axis of the tube. The tensile strength in the 90° material direction reported in Table 2 for the carbon fiber composite is in the same material direction and perpendicular to the crush tube axis.

Damage to the composite due to bending was due to general matrix fracture of the composite as it was forced over the fillets of the crush trigger. Fracture of the composite occurs when the in-plane tension loads exceed the tensile strength of the composite. The tensile strength of the composite is usually determined by the fiber strength, which is significantly higher than the resin matrix. As the composite tube sides are forced over the trigger fillets, bending causes tensile force in the 0° direction on the inside of the tube adjacent to the trigger and compressive loading on the outside of the tube. Because the fiber is significantly stronger in tension than the matrix, the matrix cracks and delamination occurs. The damage to the matrix prevents the transfer of load between fibers and the fibers are unloaded. As a result, there is fiber fracture at the tube corners where high tensile loads are imposed. The bending loads are sufficient to cause widespread matrix fracture between fibers with little fiber damage observed in the tube sides resulting in the loss of structural integrity of composite material.

Energy absorption due to friction was inferred by the physics of the crush tube test. It is readily observed that the composite is forced to slide over the trigger fillets, sides and base.



Figure 6 Quasi-statically compressed carbon fiber tube showing delamination, corner splitting and matrix damage due to bending.



Figure 7 Dynamically compressed carbon fiber composite crush tube showing delamination, corner splitting and matrix damage due to bending.

Microscopic Damage Modes

Matrix damage occurs as the result of bending of the composite as the composite crush tube is forced against a flat platen or over a plug trigger. As the composite is crushed, bending forces cause the polymer matrix to fracture. Additional microscopic damage modes such as fiber/matrix debonding and fiber/matrix pullout are probably present. These damage modes are not examined in this research effort, as each microscopic damage mode may be present with or are a part of more than one macroscopic energy absorption mode confounding efforts to isolate and measure energy absorption by each microscopic damage mode.

Characterization of Individual Damage Modes

Quantification of energy absorption by mode, is difficult because of the coupling among energy absorbing modes. During crush, the peak load is determined by the force required to fracture the carbon tows in the corner regions of the crush tube. At load levels below the strength of the carbon corner tows, other damage occurs in the composite tube such as delamination and matrix damage due to bending. Energy absorption due to sliding friction is dependent on the load normal to the sliding surface and coefficient of friction between the composite and the plug trigger surface.

The local load maximums that occur during tube crush, such as shown in Figure 5, suggest that not all energy absorption modes are occurring simultaneously. If this is so, it should be possible to isolate and measure energy absorption modes

After energy absorption modes are identified, a test must be designed that will isolate and measure each mode or groups of energy absorption modes. It is hypothesized that the energy absorption due to friction mechanisms is one of the primary modes of energy absorption for composite materials. It is further hypothesized that the difference in friction energy absorption under quasi-static loading vs. dynamic loading is the primary reason that the SEA of a composite varies depending on loading speed.

General SEA Calculation

Testing of crush tubes is accomplished by crushing the tube between the platens of a test machine in a controlled manner. Displacement and load data obtained in this type of test is used to calculate SEA. SEA is calculated by integrating the load-displacement curve to determine total energy absorbed and then dividing the total energy absorbed by the mass of the crushed portion of the tube. The mass of the tube that is crushed is determined by calculating the volume of the tube that is crushed and then multiplying the crush volume by the composite density. The crush volume was determined by multiplying the cross section area by the measured displacement obtained during testing. The cross section area of the tube is calculated using measurements of the cross section geometry.

Crush Tube Energy Absorbing Modes

A typical carbon fiber composite crush tube specimen was presented in Figure 6. Note that there is fracture of the composite at the corners and damage of the resin matrix. The flat portions of the tube between the corners have extensively damaged resin matrix resulting in a loss of bending stiffness of the composite. Also visible is delamination of the two plies of the carbon fiber composite tube.

Corner Splitting

The most apparent energy mode observed is fracture of the crush tube at the four tube corners. Examination of the carbon fiber tubes reveals fracture of the fiber tows occurs only at the four corners of the tube for both quasi-static and dynamic loading. While the composite matrix is damaged extensively in the crushed region of the tube, no fractured fiber tows were observed in the flat sides of the tube.

The fractures in the crush tube corners are similar to those observed in the 90° tensile tests. The energy density at fracture measured at 0.475 J/cm³ for the carbon fiber composite (Table 1). Strain energy density is determined by mathematically integrating strain over the affected material volume.

The total corner splitting energy absorption of the crush tube is calculated by multiplying the tube corner volume by the tensile strain energy density at fracture. The SEA attributable to corner splitting energy is calculated by dividing total corner splitting energy by the total mass of the crushed tube. The corner splitting SEA is presented in Table V.

Table V | Carbon fiber composite corner splitting SEA.

Tube #	Corner Area (cm ²)	Crush Length (cm)	Fracture Energy (J/cm ³)	Tube Crush Mass (gm)	SEA (J/gm)
4278-2-1	1.01	12.4	0.475	92.0	0.065
4278-2-4	0.90	12.4	0.475	85.4	0.062
4278-2-5	0.86	12.4	0.475	86.0	0.059
4278-2-9	0.91	12.4	0.475	86.3	0.062
4278-2-17	0.97	12.4	0.475	86.1	0.066
Average	0.93	12.4	0.475	87.2	0.063

Delamination

Delamination was evident when the carbon composite tubes were crushed. Calculation of the energy absorbed by this damage mechanism was determined using the Mode 2 critical strain energy release rate, G_{IIc} using the end notch flexure test [Ref. 7]. The value of G_{IIc} of the carbon fiber composite is presented in Table I. Multiplying G_{IIc} by the surface area that is created during tube crush and dividing by the mass of the crush tube that is crushed results in a value for the SEA for this mode. Note that there are two surface created in the carbon fiber composite tube by delamination. The delamination test results are presented in Table VI.

Table VI Carbon fiber composite SEA due to delamination.

Coupon	G_{IIC} (J/cm ²)	Delaminated Surface Area (cm ²)	Crushed Tube Mass (gm)	SEA (J/gm)
4278-2-1	0.164	451	92.5	0.798
4278-2-4	0.164	450	85.9	0.857
4278-2-5	0.164	449	86.5	0.850
4278-2-9	0.164	450	86.8	0.848
4278-2-17	0.164	451	86.6	0.852
			Average:	0.841

Note: SEA based on material density of 1.42 gm/cm³.

Matrix Fracture Due to Bending and Friction

Matrix damage due to resin fracture is the second energy absorption mode that was observed. Figures 6 and 7 show that the flat sides of the crush tube have been forced to follow the radius of the plug trigger. The crush tube sides are thus deformed into a curved petal shape. The stiffness of the petals has been reduced to the point that the crushed petals can be deformed easily whereas the undamaged sides of the crush tube remain rigid. As the fibers in the petals are not fractured, the only composite component observed to be damaged is the resin. Close examination of the damaged composite shows that the resin has fractured into very small granules that remain attached to the fiber tow bundles. At the edges of the composite petals, individual fiber tow bundles are observed to be free from the petals. The fiber tows can be easily separated from the damaged composite showing extensive damage of the resin matrix and loss of continuity between the fiber tows. This characteristic of the damaged composite was consistent between the quasi-static and dynamic tested specimens.

The SEA attributable to friction and matrix damage due to bending was determined using a novel strip test fixture designed by the author. The test fixture and procedure is presented in [Ref 8]. A schematic of the test fixture is presented in Figure 8.

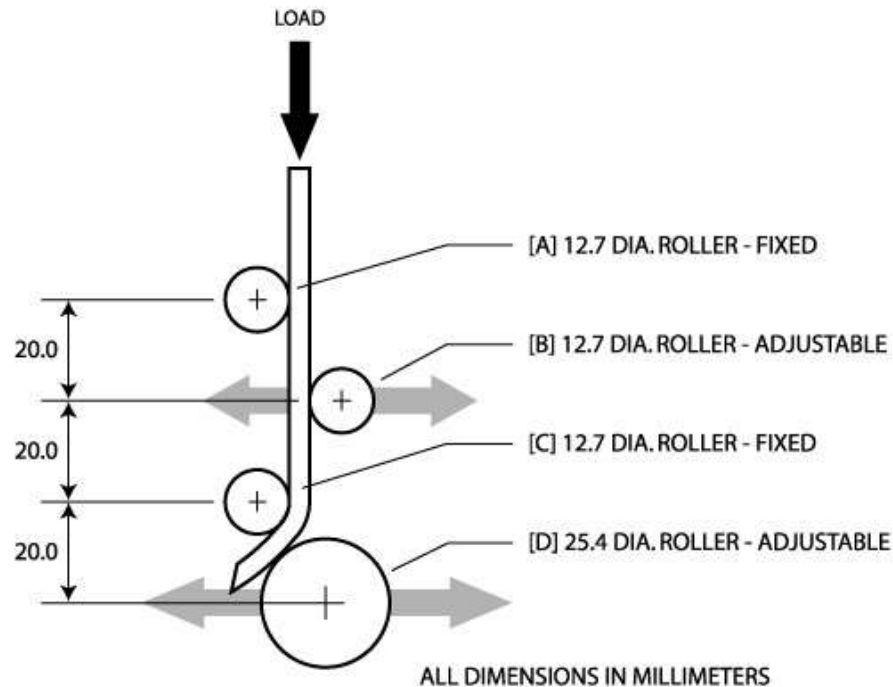


Figure 8 Strip test fixture schematic.

A summary of strip testing is presented in Table VII. The variables presented are load speed and roller D fixity. The first comparison can be made for cases with varied load speed and locked roller D. When the loading is quasi-static (case 1), the average SEA is 19.3 J/m. When the loading is dynamic, either at 2.0 m/sec (case 3) or 0.5 m/sec (case 5), the average SEA is 15.4 J/m, a 20% reduction compared with the quasi-static result.

When the roller D is free to rotate there was little difference observed in the SEA between quasi-static loading (13.3 J/gm of case 2) and dynamic load rate is 2.0 m/sec (13.0 J/gm in case 4).of There was only a slight difference in SEA when the dynamic load rate of 0.5 m/sec (13.3 J/gm in case 6). This result and the results described in the previous two paragraphs clearly demonstrate that:

Sliding friction absorbs a significant amount of energy at least in quasi-static cases.

Energy absorption due to sliding friction can be separated from those due to damage formation.

The difference in SEA between quasi-static and dynamic loading is due to the change in sliding friction SEA when loaded at a quasi-static load rate vs. a dynamic load rate.

Table VII Strip test results summary.

Case	Crush Speed	Roller D Fixity	Average SEA (J/gm)
1	Quasi-Static	Locked	19.3
2	Quasi-Static	Free	13.3
3	2.0 m/sec	Locked	15.4
4	2.0 m/sec	Free	13.0
5	0.5 m/sec	Locked	15.4
6	0.5 m/sec	Free	13.3

Energy Balance

The minor energy absorption modes, corner splitting and delamination, were quantified using simple mechanical tests for quasi-static loading. Dynamic energy absorption was not measured for corner splitting and delamination because strain rate effects suggest that the SEA would increase slightly. Weeks and Sun, [Ref 9], and Todo, [Ref 10], report an increase in tensile strength of 20-25 MPa per order of magnitude increase in strain rate, and the relative magnitude of corner splitting SEA and delamination SEA is small. Corner splitting accounted for only 0.21% (0.063 J/gm) of the quasi-static SEA. Delamination accounted for 2.7% (0.84 J/gm). The remaining 97%, 29.5 J/gm (Table IX) was attributed to sliding friction and matrix damage due to bending. The strip test results provide a good estimate of energy absorption due to sliding friction and bending.

A summary of energy absorption of strips and tubes during quasi-static loading is presented in Table VIII. The energy absorbed in the strip test with quasi-static loading and locked roller D was 19.3 J/gm. The SEA attributed to sliding friction and damage due to bending in a carbon composite crush tube was 29.5 J/gm. The difference of 10.2 J/gm can be attributed to the reduced damage observed in the strips. The appearance of the damaged strips does not show the degree of matrix damage seen in tubes. A limitation of the strip test is the larger radius that the composite strip is forced over during the strip test compared with the tube crush tube. The strip test fixture is limited to bending the strip over a minimum radius of 6.3 mm, the radius of roller C. In addition, the test specimens were twice the thickness of the composite crush tubes (4 mm vs. 2 mm). The deformation radius of the outside of a strip is at least 10 mm when the minimum inside radius is 6 mm. When the carbon composite tube is forced over the standard trigger, the maximum bending radius of the composite is the radius of the plug trigger, 6 mm. The minimum bending radius is smaller by the thickness of the 2 mm thick composite, or 4 mm. Thinner specimens could not be tested with the strip test fixture due to test coupon structural instability. The important information obtained from the strip test described is the ratio of SEA due to sliding friction compared with SEA due to bending.

There is one additional adjustment to the calculation of friction and bending SEA that must be made due to the increased thickness of the strip used in the strip test. The material used for strip testing was taken from a plaque that was twice the thickness containing twice the number of braided plies. This means that there are three delamination planes compared with the one delamination plane of the carbon composite tubes. Thus, the SEA value for delamination for the strip test is 2.52 J/gm or three times the delamination value for carbon composite tubes, 0.84 J/gm. This delamination SEA value of 2.52 J/gm was subtracted from the quasi-static load rate, locked roller D strip test SEA of 19.3 J/m (Table VIII), giving a sliding friction plus bending damage SEA value of 16.8 J/gm. The sliding friction and bending SEA values were then calculated and tabulated in the second column of Table VIII.

The friction and bending SEA for the carbon composite tubes loaded quasi-statically was determined to be 97% of the tube SEA or 29.5 J/m. This value was divided by the strip friction plus bending damage SEA of 16.8 J/gm to obtain a ratio to quantitatively determine the friction and bending SEA for carbon composite tube crush. These values are presented in the third column of Table VIII. Because friction is dependent upon the crush load which is affected by the bending strength as well as the delamination and corner splitting forces required for progressive crush, the ratio of sliding friction SEA to bending SEA is assumed to not vary between the strip test results and the tube crush results. Note that friction is determined to account for 10.6 J/gm or 34.8 % of the energy absorbed when the carbon composite tubes are crushed at the quasi-static rate.

Determination of the dynamic crush energy balance for strips and crush tubes was determined in a similar manner and is presented in Table IX. The energy absorption due to bending was essentially unchanged (10.8 J/gm vs. 10.4 J/gm). Dynamic energy absorption due to sliding friction decreased significantly, 4.26 J/gm vs. 10.6 J/gm for quasi-static loading. Compare this reduction in SEA due to sliding friction of 6.34 J/gm with the overall reduction in carbon composite tube crush SEA from 30.4 J/gm for quasi-static load rate to 23.8 J/gm for dynamic load rate, a reduction of 6.6 J/gm. It can be concluded that for this composite system, nearly all of the measured SEA reduction when the load rate is changed from quasi-static to dynamic, 2.0 m/sec, is attributable to sliding friction. A summary is presented in Table X.

Table VIII Carbon composite strip and crush tube energy balance with quasi-static loading.

Energy Mode	Strip		Tube	
	J/gm	%	J/gm	%
Delamination + Bending	13.3	68.9	--	
Friction + Bending	16.8	87.0	29.5	97.0
Delamination	2.5	13	0.84	2.8
Bending	10.8	56	18.9	62.2
Friction	6.0	31	10.6	34.8
Corner splitting	0.0	0.0	0.06	0.2
Total	19.3	100	30.4	100

Table IX Carbon composite strip and crush tube energy balance dynamic loading (2.0 m/sec).

Energy Mode	Strip		Tube	
	J/gm	%	(J/gm)	%
Delamination + Bending	13.0	84.4	--	
Friction + Bending	12.9	83.8	22.9	
Delamination	2.5	16.2	0.84	3.5
Bending	10.5	68.2	18.6	78.1
Friction	2.4	15.6	4.3	18.1
Corner splitting	0.0	0.0	0.06	0.3
Total	15.4	100	23.8	100

Tabl IX Quasi-static vs. dynamic loaded carbon composite tube crush dynamic load rate (2.0 m/sec).

Energy Mode	Quasi-Static		Dynamic		Difference	
	J/gm	%	J/gm	%	J/gm	%
Delamination	0.84	2.8	0.84	3.5	0	0
Bending	18.9	62.2	18.6	78.1	-0.3	5
Friction	10.6	34.8	4.3	18.1	-6.34	96
Tube Corner splitting	0.063	0.2	0.06	0.3	0	
Total	30.4	100	23.8	100	-6.6	100

Conclusions

Carbon fiber/vinyl ester composite crush tubes were investigated with quasi-static and dynamic compression and energy absorbing modes were identified. The observed energy absorbing modes included: tube corner splitting, composite delamination, matrix damage due to bending, and sliding friction of the composite with the plug type crush trigger.

Energy absorption attributable to corner splitting at quasi-static compression was estimated using standard tensile test results. Corner splitting was estimated to absorb less than 1% of the total energy absorbed by the carbon fiber composite crush tubes.

Energy absorption attributable to delamination was estimated using the mode II (shear mode) strain energy release rate obtained using the end notch flexure (ENF) test. Under quasi-static compression, the delamination SEA was found to be 0.84 J/gm or 2.8% of the total tube SEA.

An innovative strip test fixture was designed and fabricated to separate the sliding friction SEA from the SEA attributable to matrix damage due to bending. Carbon fiber composite SEA, under quasi-static compression, attributable to matrix damage due to bending was found to be 18.9 J/gm or 62.2% of the total tube SEA. Under dynamic crush, the SEA attributable to matrix damage due to bending was found to be 18.6 J/gm or 78.1% of the total tube SEA.

Carbon fiber composite SEA attributable to sliding friction under quasi-static compression was found to be 10.6 J/gm or 34.8% of the total tube SEA. Under dynamic crush, the SEA attributable to sliding friction was found to be 4.3 J/gm or 18.1% of the total SEA. The decrease in sliding friction SEA of 6.3 J/gm accounted for nearly all of the decrease in tube SEA of 6.6 J/gm between dynamic crush and quasi-static compression. Sliding friction was concluded to be responsible for the decrease in overall tube SEA from quasi-static compression to dynamic crush.

Acknowledgements

The author would like to acknowledge and thank the contributions of the following individuals and organizations for support of this research:

The technical fabricators of the Ford Scientific Research Laboratory shop, Paul Ostrander and Gary Fleming, for the fabrication of and their design suggestions of the strip test fixture.

Mike Starbuck and Rick Battiste of Oak Ridge National Laboratory, National Transportation Research Center, for conducting dynamic load tests.

Dan Houston and Ron Cooper of the Ford Scientific Research Laboratory for performing quasi-static crush tests.

Nancy Johnson and Ruth Gusko of the GM Research Center for plaque and crush tube fabrication.

I would also like to acknowledge and thank the DOE program management team and the Board and staff of the Automotive Composites Consortium. This work was sponsored by the Automotive Composites Consortium and the U. S. Department of Energy, Office of Transportation Technologies, Office of Advanced Technologies, Lightweight Materials Program under Cooperative Agreement number FC05-02OR22910.

References

1. Chadwick, M. M. and Caliskan, A. G., "Fracture Mechanisms Observed in Crush of Vinyl Ester-Glass Composite Tubes", Private Communication, 1998
2. Farley, Gary, Jones, Robert, "Analogy for the Effect of Material and Geometrical Variables on Energy-Absorption Capability of Composite Tubes", Journal of Composite Materials **26** (1992) 78-89
3. Thornton, P.H., "Energy Absorption in Composites", Proc SEM Spring Conference on Experimental Mechanics, June 709, 1993, Dearborn, MI
4. Mamalis, A. G., Manolacos, D.E., Demosthenous, G. A., Ioannidis, "The static and dynamic axial collapse of fiberglass composite automotive frame rails", Composite Structures **34** (1996) 77-99
5. ASTM D2584-02 Standard Test Method for Ignition Loss of Cured Reinforced Resins
6. Delsen Test Report T 37674, 07/23/03
7. End Notch Flexure of Fiber Reinforced Composites, General Electric Specification No 4013367-059, Issue 2.
8. Brimhall, T. J., "Measurement of Static and Dynamic Friction Energy Absorption in Carbon Vinyl ester Composite", S.P.E, Advanced Composites Conference and Exposition, Sept. 2006.
9. Weeks, C.A., Sun, C. T., "Modeling Non-Linear Rate-Dependent Behavior in Fiber-Reinforced Composites", Composites Science and Technology **58** (1998) 603-611, Elsevier Science Limited, Great Britain
10. Todo, M., Takahashi, K., Beguelin, P., Kausch, H. H., "Strain-rate dependence on the tensile fracture behavior of woven-cloth reinforced polyamide composites", Composite Science and Technology **60** (2000) 763-771, Elsevier Science Limited, Great Britain